Available online at www.sciencedirect.com
ScienceDirect
Optical Materials 30 (2007) 502–507
OPTICAL Materials
www.elsevier.com/locate/optmat

Correlation between photoluminescence and varied growth pressure of well-aligned ZnO nanorods on fused silica substrate

Song Yang [a], Hsu-Cheng Hsu [b], Wei-Ren Liu [a], Hsin-Min Cheng [a], Wen-Feng Hsieh [a,*]

[a] Department of Photonics, Institute of Electro-Optical Engineering, National Chiao Tung University, 1001 Tahsueh Road, Hsinchu 30050, Taiwan
[b] Center for Condensed Matter Sciences, National Taiwan University, Taipei 106, Taiwan

Received 12 September 2006; received in revised form 5 January 2007; accepted 12 January 2007
Available online 28 February 2007

Abstract

Well-aligned ZnO nanorods with variable diameters were fabricated on fused silica substrates by the simple physical vapor deposition method with and without pre-deposited NiO particles. The diameter control of ZnO nanorods on the fused silica substrates was achieved by varying the growth pressure. The room-temperature photoluminescence spectra of the ZnO nanorods exhibit strong exciton emission at 3.25 eV that reveals good crystal quality. The exciton emission peak shifts toward 3.22 eV for the samples made at the larger growth pressure that is attributed to the influence of the electron-acceptor-level transition. The ZnO nanorods were examined by high resolution transmission electron microscopy and X-ray diffraction to show single crystal quality and preferentially *c*-axis alignment. Furthermore, we used scanning electron microscope to verify not only the size but also the growth mechanisms of ZnO nanorods. The results show a ZnO buffer layer formed between the flat top-facet nanorods and the substrate. In comparison with the samples without pre-deposited NiO particles on the substrate, the pre-deposited NiO particles act as nucleation centers for Zn vapor during the deposition process that improves the quality of the buffer layer.

PACS: 61.10.−i; 71.55.Gs; 73.61.Tm; 78.55.Et

Keywords: Zinc oxide; Nanorods; Nanowires; Photoluminescence; Silica; Pressure

1. Introduction

ZnO has some of the greatest potential among semiconductor materials for applications in ultraviolet regions and nanotechnology. It has a wide direct bandgap of about 3.37 eV at room temperature, and large exciton binding energy of about 60 meV. These properties allow it to emit ultraviolet light with high efficiency at room temperature, and give it superiority in many applications. For instance, ZnO thin film structures can be utilized as piezoelectrical device and ultraviolet light emitting diode [1]. Recently, large second order susceptibility (up to 56 pm/V), which is a crucial technological parameter, had been measured in ZnO films deposited on MgO substrates [2]. The nano-confined effect and interface separating substrate and the nanoparticles play the major role on the large optical non-linearity in these ZnO films. For low-dimensional ZnO nanostructures, ZnO nanoparticles or quantum dots have attracted much research attention in fundamental studies and technical applications because of their unusual characteristics [3]. Besides, ZnO had been made into solar cells using nanorods [4] and nanoparticles [5], nano logic circuit [6], nano laser source [7], and field emission device [8] have been studied using one-dimensional (1D) ZnO nanostructures, which can be fabricated on various substrates such as Si [9–12], sapphire [13,14], Al_2O_3 [15], silica [16], etc.

It is very important for fabricating nano-photonic devices in 1D nanostructures with well control of diameter.

* Corresponding author. Tel.: +886 3 5712121x56316; fax: +886 3 5716631.
E-mail address: wfhsieh@mail.nctu.edu.tw (W.-F. Hsieh).

0925-3467/$ - see front matter © 2007 Elsevier B.V. All rights reserved.
doi:10.1016/j.optmat.2007.01.004

Yang et al. [9] reported that the diameters of the ZnO nanorods should depend on the size of the catalyst, gold nanoparticles, in a vapor–liquid–solid growth mechanism. Lee et al. [15] reported that the diameter can be controlled by the growth temperatures in a limit range. By varying the growth ambient pressure, diameter-controlled Si nanowires of 6–25 nm were reported [17]. For the potential of photonic application and of merging with the Si-based technologies, in this paper, we fabricated well-aligned ZnO nanorods by using the simple physical vapor-deposition method [15] on silica substrates and showed that the mean diameter of ZnO nanorods can be varied by the ambient pressure inside the furnace tube. The room-temperature photoluminescence (PL) properties of the samples were investigated to realize the growth pressure dependence of the ZnO nanorod quality. Furthermore, the growth mechanism is also discussed.

2. Experimental

The ZnO nanorods were fabricated by the following procedure: The 0.01 M $Ni(NO_3)_26H_2O$ dissolved in ethanol was sprayed on a clean fused silica substrate. After baking for 5 min in air on a hotplate at 60 °C, the substrate was loaded 2 cm above an alumina boat that contains 1 g metal zinc balls (99.999% with 1–3 mm in diameter). Then the boat was placed in the center of a quartz tube furnace. After evacuating the tube by a mechanical pump, argon gas was introduced into the tube with a flow rate of 50 sccm. Then the tube was heated at the rate of 20 °C/min to the reaction temperature of 600 °C, and maintained for 30 min at the ambient pressures of 50 Torr. Finally, the furnace was cooled to room temperature at cooling rate of about 100 °C per hour, and the gray wax-like product was found on the substrate surface.

A 20-mW He–Cd laser (Omnichrome 74 Series), radiated at 325 nm, was used as the excitation source for the PL measurement at room temperature. The emitted light was collected by a Triax 320 spectrometer equipped with a UV-sensitive photomultiplier tube. The morphology and crystal structure of the product were characterized by field emission scanning electron microscopy (FESEM), high resolution transmission electron microscopy (HRTEM), and X-ray diffraction (XRD).

3. Results and discussion

3.1. Photoluminescence

The power of about 20-mW from the He–Cd laser (Omnichrome 74 Series) was used to excite the samples in the PL measurement. Fig. 1a shows a room-temperature PL spectrum of the ZnO nanorods that were grown at the ambient pressures of 50, 100, 110, and 150 Torr, respectively. As the ambient pressure increases over 100 Torr, the strong near bandedge (NBE) peak, which is attributed to the exciton emission, starts to red-shift from 3.25 eV to 3.22 eV with its FWHM being broadened from 111 meV to 164 meV. The inset of Fig. 1a shows the relatively weak broadband emission at about 2.54 eV with large FWHM of ~770 meV. The FWHM and the peak position of the NBE emission versus the growth pressure are shown in Fig. 1b. The FWHM increases obviously with increasing ambient pressure when the pressure exceeds 100 Torr; meanwhile, the peak position starts to red-shift.

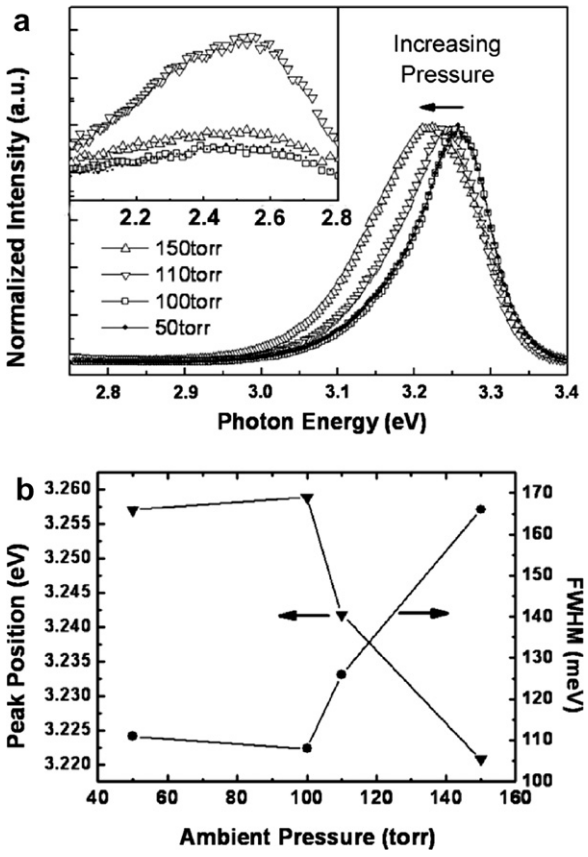

Fig. 1. (a) The room-temperature PL spectrum of the ZnO nanorods grown at the ambient pressure of 50, 100, 110 and 150 Torr, and the weak broadband emission at about 2.54 eV inside the inset picture. (b) The FHWM and the peak position of the strong emission depending on the ambient pressures.

From the PL spectra, the samples formed at less than 100 Torr ambient pressure have a strong NBE emission, with peak position at about 3.25 eV. The red-shifting behavior of the NBE emission at room temperature for the ambient pressure beyond 100 Torr is attributed to the defect influence. The defects in the ZnO produce the electron-acceptor-level transition emission (eA^0) and lead the NBE peak position to vary from 3.22 eV to 3.25 eV. This was attributed to the overlap of the 3.31 eV (due to free exciton emission) and 3.23 eV (due to eA^0) [14,18]. The acceptor could be the Zn vacancy because, in the experiment procedure, there was no any acceptor source except for the Zn vacancy. The red-shifting behavior implies that the acceptor density increases with the growth pressure. The acceptor could be attributed to the turbulent flow

condition, which could disturb the crystal growth process and result in the Zn vacancy appearance; the acceptor density depends on the turbulent flow degree.

3.2. Technological details

In order to verify dependence of PL on diameter of ZnO nanorods under various growth pressures, we used SEM to characterize our samples under different growth conditions. We also compared the growth mechanisms with and without pre-coated NiO particles in this section.

Fig. 2a shows the SEM top-view of the ZnO nanorods that were synthesized at 600 °C and 50 Torr ambient pressure. The ZnO nanorods reveal flat tip facet with no NiO particles on top with their diameters ranging between 100 and 200 nm and density of about 3.3×10^8 cm^{-2}. Fig. 2b is the cross-section image of the sample. From this image, a 2-μm thick ZnO buffer layer was observed between the ZnO nanorods and the fused silica substrate. The ZnO nanorods are well aligned on the buffer layer and have a mean diameter of ~130 nm and length of ~5 μm. The ZnO nanorods on the buffer layer have a slight tilt to the substrate surface and reveal slightly larger diameters at the root of the nanorods close to the buffer layer. The HRTEM image (Fig. 2c) shows that the ZnO nanorods have *c*-axial grown single-crystalline structure. The inset of Fig. 2c is the selected area electron diffraction pattern of (11–20) zone axis of ZnO nanorods that reveals a single-crystalline structure of ZnO nanorods. These results reveal that high-crystalline structured ZnO nanorods were successfully synthesized.

Fig. 2d is the θ–2θ XRD scan data of the as-grown ZnO products on the silica substrate. Since The XRD structure is analyzed within a framework of the bulk-like structure, contribution of the nano-sized sheet (buffer layer) may be present in the XRD data. The strongest peak at 34.5° and two relatively smaller peaks at 31.58° and 36.1° were identified as ZnO (002), (100), and (101) crystal planes, respectively. The results indicate that the ZnO nanorods were grown with a *c*-axis orientation that is perpendicular to the substrate surface. The lattice constants of $a = 3.269$ Å and $c = 5.195$ Å (bulk ZnO: $a = 3.249$ Å and $c = 5.206$ Å, according to JCPD-36-1451) were calculated from the XRD scan data.

In order to investigate the influence of the NiO particles on growth of nanorods, we made two samples at the same condition (fabricated at 600 °C and 50 Torr ambient pressure); one was coated with NiO particles on the substrate surface, and the other was not. From the XRD θ-rocking curve measurement in Fig. 3a and b, the degree of nanorod alignment to the normal direction of the substrate surface was indicated [19]. Fig. 3a shows the XRD θ-rocking curve measurement of the sample coated with NiO particles on the substrate and indicates the full width at half maximum (FWHM) value of 9.24°, whereas, FWHM value of 12.18° in Fig. 3b for the sample without pre-coated NiO particles. This comparison implies that the degree of nanorod alignment of the sample with NiO particles is better than the sample without NiO particles.

As mentioned above, since no NiO particles on the tip of the ZnO nanorods that suggests the NiO particles do not act as catalysts of the vapor–liquid–solid (VLS) mechanism

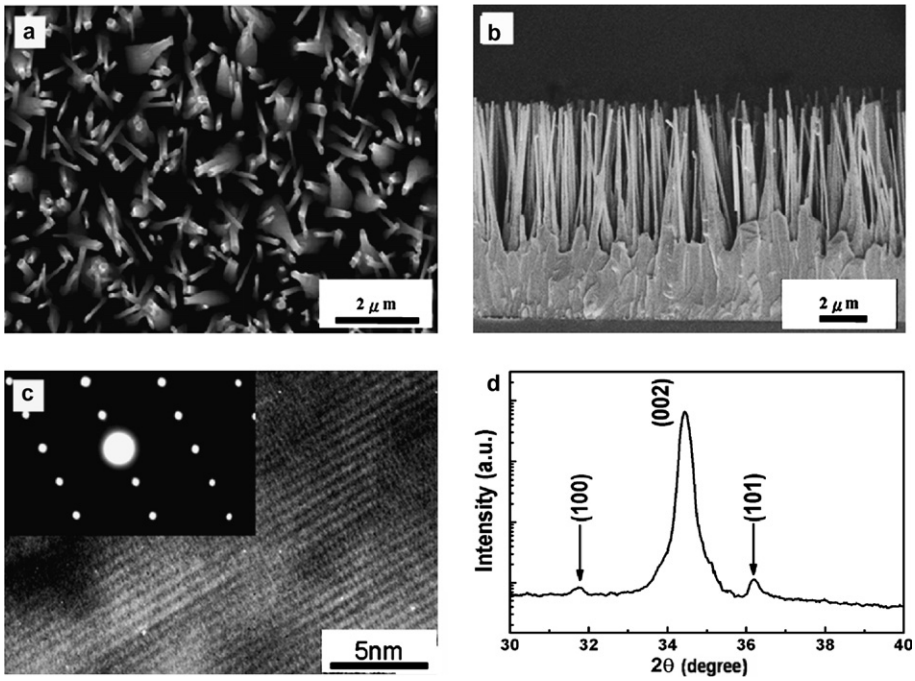

Fig. 2. The ZnO material synthesized at 600 °C and 50 Torr ambient pressure shows (a) the top-viewed SEM image, (b) the cross-section SEM image, (c) the HRTEM image with inset image showing the selected area electron diffraction pattern of (11–20) zone axis in ZnO nanorods, (d) and the θ–2θ XRD scan data.

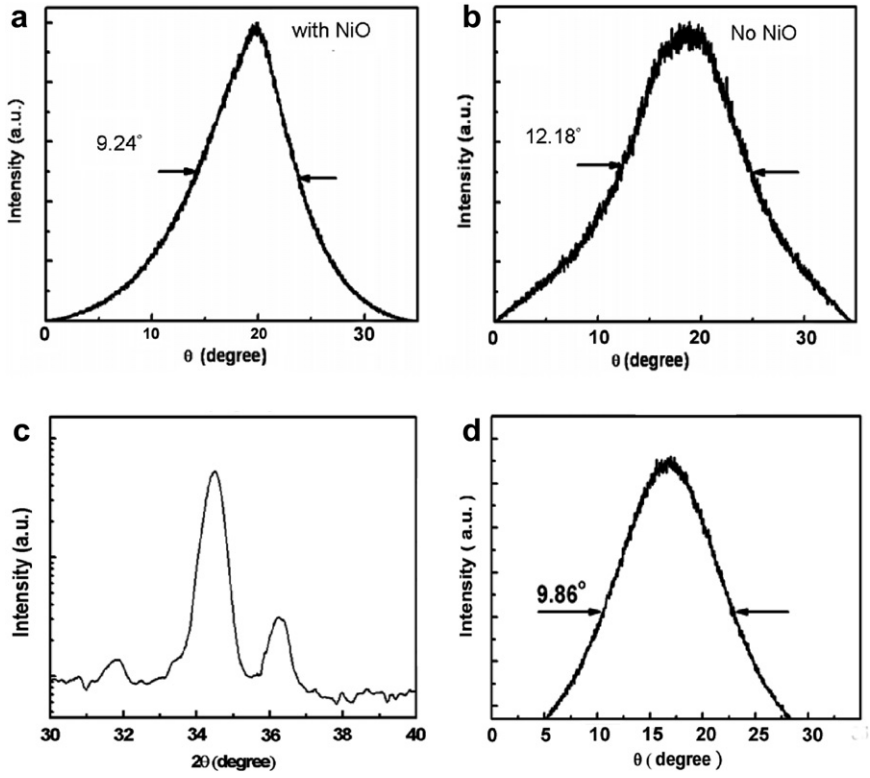

Fig. 3. The XRD θ-rocking curve measurement of the two samples both made at 600 °C and 50 Torr. (a) One had coated with NiO particles on the substrate surface and (b) the other had not. The grazing incident X-ray diffraction (GID) (c) and rocking curve (d) of the ZnO buffer layer.

[9]. The NiO particles probably were covered under the ZnO buffer layer, and the ZnO nanorods follow a catalyst-free growth model [15]. In the initial deposition stage, the NiO particles may act as the centers of the nucleation that induce the Zn vapor to condense and react with the residual oxygen in the furnace tube. Therefore, the ZnO_x with $x < 1$ may be formed around the NiO particles. Due to the low melting point of ~490 °C for ZnO_x [20], the melting ZnO_x cannot only move around but also further react with the residual oxygen. Then the ZnO_x becomes ZnO and forms a rough ZnO buffer layer during the grown temperature increase. Finally the *c*-axis vertically aligned ZnO nanorods started to grow on the $\langle 0\,0\,1\rangle$ prefer-oriented rough ZnO buffer layer. The ZnO buffer layer formed under such a condition should have a rough crystalline quality, due to the amorphous substrate and NiO crystalline orientation on the amorphous substrate. While the ZnO nanorods start to grow, the orientation of nanorods would depend on the quality of the ZnO buffer layer and have a slight tilt to the substrate surface. To investigate the tilt orientation of the buffer layer, the sample had been polished to remove the ZnO nanorods. Two measurements were taken of the buffer layer—grazing incident X-ray diffraction (GID) in Fig. 3c and rocking curve in Fig. 3d. These two measurements indicated the polycrystalline quality and growth orientation, which had a slight misalignment with the *c*-axis.

The oblique-view SEM images of Fig. 4a and b show the obvious difference in the size of the ZnO nanorods that were grown at different ambient pressures of 50 and 150 Torr, respectively. The mean diameters and corresponding deviations of the ZnO nanorods grown at a series of different ambient pressures (10–150 Torr) were estimated in Fig. 4c. It was observed that the mean diameters of the ZnO nanorods increase as a function of the ambient pressure. The mean diameter of the ZnO nanorods nearly equals 130 nm below the ambient pressure at 100 Torr, and shows a tendency to increase with the increasing ambient pressure above 100 Torr. This result implies some kind of relationship between the pressure and the size of the nanorods. The gas flow condition during the reaction process would strongly influence the dimension and the quality of the ZnO nanorods in the vapor deposition process. In our vapor deposition process, the ambient pressure in the reaction tube is controlled by the evacuation rate, using a mechanical pump while keeping constant Ar-gas flow rate. The NiO particles probably would lead the ZnO buffer layer to grow grain by grain, with randomly grown ZnO nanorods showing increasing diameters as the ambient pressure in the tube furnace increases. The flow condition can be indicated by the Reynolds number (*Re*): $Re = (Dv\rho)/\mu$, where D is the characteristic length (determined by the diameter of reaction tube and shape of the boat), v is the fluid velocity, ρ is the fluid density, and μ is the fluid viscosity. The larger ambient pressure makes the larger fluid density, and the flow condition may transfer from the laminar flow to the more turbulent flow even with the constant Ar-gas flow rate. For this reason, the Zn

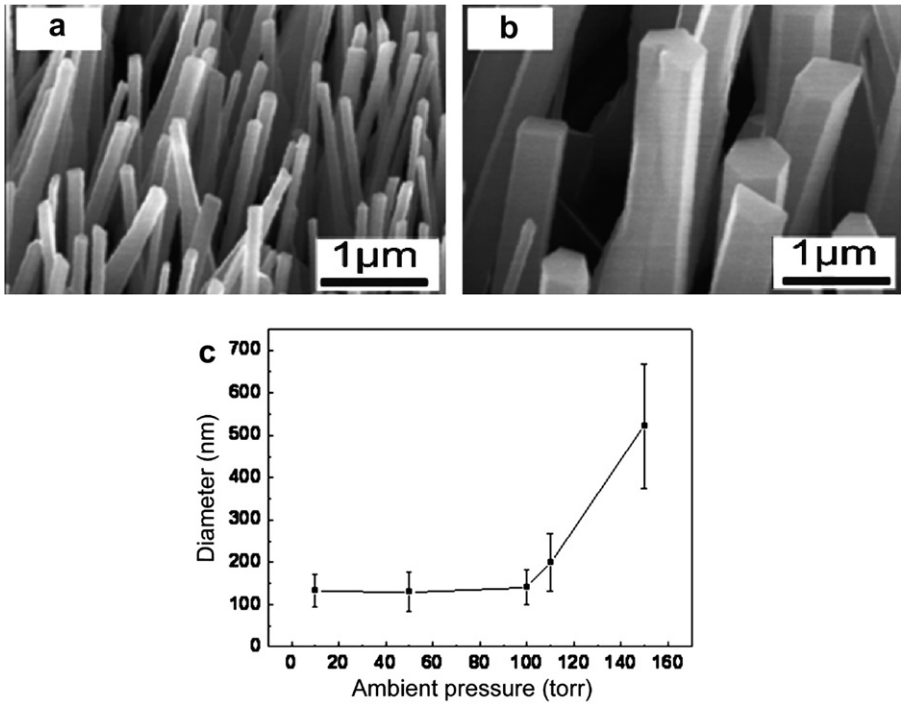

Fig. 4. The oblique-view SEM images of the ZnO nanorods grown at (a) 50 Torr and (b) 150 Torr, and (c) the mean diameters and corresponding deviations of the ZnO nanorods grown at a series of different ambient pressures (10–150 Torr).

vapor atoms flowing with Ar-gas would more frequently and turbulently collide with the substrate surface at the higher ambient pressure. This condition increases the probability of contacting the side plane of the ZnO nanorods and benefits the increasing of the ZnO nanorods diameter. The influence of the ambient pressure also had been discussed on the diameter of Si nanorods ranging from 150 to 600 Torr [17].

4. Conclusion

The well-aligned ZnO nanorods were successfully fabricated on the amorphous fused silica substrate. From the preceding investigation, the alignment of the nanorods on the amorphous substrate was attributed to the buffer layer that was studied by the GID and rocking-curve measurement. The HRTEM and XRD patterns indicated that the as-grown ZnO nanorods have wurtzite structure and good single crystalline quality. The analysis indicated that the function of the NiO particles in this procedure is to attract the Zn vapor and to form the ZnO buffer layer, which improves the alignment of the nanorods on the amorphous silica substrate. The XRD rocking curve indicated the degree of vertical alignment of the ZnO nanorods. The diameters of the ZnO nanorods were related to the ambient pressure in the vapor deposition process. We could take advantage of the characteristic to regulate the mean diameter of the ZnO nanorods in the range of 130–500 nm. The defect density related to the ambient pressure in the vapor deposition process. The red-shift of the emission peak was attributed to the influence of the electron-acceptor-level transition emission. The red-shift of the emission peak reflects the defect density and crystal quality of the ZnO nanorods.

Acknowledgements

The authors would like to thank Mr. C.C. Lin for help in the TEM measurement. This work was partly supported by NSC of the Republic of China under Contract No. NSC 94-2112-M-009-015.

References

[1] A. Tsukazaki, A. Ohtomo, T. Onuma, M. Ohtani, M. Sumiya, K. Ohtani, S.F. Chichibu, S. Fuke, Y. Segawa, H. Ohno, H. Koinuma, M. Kawasaki, Nat. Mater. 4 (2005) 42.
[2] J. Ebothe, I.V. Kityk, S. Benet, B. Claudet, K.J. Plucinski, K. Ozga, Optics Commun. 268 (2006) 269.
[3] K.F. Lin, H.M. Cheng, H.C. Hsu, L.J. Lin, W.F. Hsieh, Chem. Phys. Lett. 409 (2005) 208.
[4] M. Law, L.E. Greene, J.C. Johnson, R. Saykally, P.D. Yang, Nat. Mater. 4 (2005) 455.
[5] W.J.E. Beek, M.M. Wienk, R.A.J. Janssen, J. Mater. Chem. 15 (2005) 2985.
[6] W.I. Park, J.S. Kim, G.C. Yi, H.J. Lee, Adv. Mater. 17 (2005) 1393.
[7] M.H. Huang, S. Mao, H. Feick, H. Yan, Y. Wu, H. Kind, E. Weber, R. Russo, P. Yang, Science 292 (2001) 1897.
[8] Y.K. Tseng, C.J. Huang, H.M. Cheng, I.N. Lin, K.S. Liu, I.C. Chen, Adv. Func. Mater. 13 (2003) 811.
[9] M.H. Huang, Y. Wu, H. Feick, N. Tran, E. Weber, P.D. Yang, Adv. Mater. 13 (2001) 113.
[10] J.S. Lee, M.I. Kang, S. Kim, M.S. Lee, Y.K. Lee, J. Cryst. Growth 249 (2003) 201.

[11] S.C. Liu, J.J. Wu, J. Mater. Chem. 12 (2002) 3125.
[12] J.J. Wu, S.C. Liu, Adv. Mater. 14 (2002) 215.
[13] Y.Y. Wu, H.Q. Yan, M.H. Huang, B. Messer, J.H. Song, P.D. Yang, Chem. Eur. J. 8 (2002) 1261.
[14] B.P. Zhang, N.T. Binh, Y. Segawa, Appl. Phys. Lett. 84 (2004) 586.
[15] S.C. Lyu, Y. Zhang, C.J. Lee, H. Ruh, H.J. Lee, Chem. Mater. 15 (2003) 3294.
[16] H. Yuan, Y. Zhang, J. Cryst. Growth 263 (2004) 119.
[17] H.Z. Zhang, D.P. Yu, Y. Ding, Z.G. Bai, Q.L. Hang, S.Q. Feng, Appl. Phys. Lett. 73 (1998) 3396.
[18] B.P. Zhang, N.T. Binh, K. Wakatsuki, Y. Segawa, Y. Kashiwaba, K. Haga, Nanotechnology 15 (2004) S382.
[19] W.I. Park, D.H. Kim, S.W. Jung, G.C. Yi, Appl. Phys. Lett. 80 (2002) 4232.
[20] B.D. Yao, Y.F. Chan, N. Wang, Appl. Phys. Lett. 81 (1998) 757.